Selectively targeting the kinome-conserved lysine of PI3Kδ as a general approach to covalent kinase inhibition

Samuel E Dalton,[†,‡] Lars Dittus,[¥] Daniel A Thomas,[‡] Máire A Convery,[‡] Joao Nunes,[‡] Jacob T Bush,[‡] John P Evans,[‡] Thilo Werner,[¥] Marcus Bantscheff,[¥] John A Murphy,[†] and Sebastien Campos[‡,*]

[†] Department of Pure and Applied Chemistry, WestCHEM, University of Strathclyde, 295 Cathedral Street, Glasgow, G1 1XL, U.K.

[‡] GlaxoSmithKline Medicines Research Centre, Gunnels Wood Road, Stevenage, Hertfordshire, SG1 2NY, U.K.

[¥] Cellzome GmbH, a GSK company, Meyerhofstr. 1, Heidelberg, 69117, Germany

ABSTRACT: Selective covalent inhibition of kinases by targeting poorly conserved cysteines has proven highly fruitful to date in the development of chemical probes and approved drugs. However, this approach is limited to ~200 kinases possessing such a cysteine near the ATP-binding pocket. Herein, we report a novel approach to achieve selective, irreversible kinase inhibition, by targeting the conserved catalytic lysine residue. We have illustrated our approach by developing selective, covalent PI3Kδ inhibitors that exhibit nanomolar potency in cellular assays, and a duration of action >48 h in CD4+ T cells. Despite conservation of the lysine residue throughout the kinome, the lead compound shows high levels of selectivity over a selection of lipid and protein kinases in biochemical assays, as well as covalent binding to very few off-target proteins in live-cell proteomic studies. We anticipate this approach could offer an alternative general strategy, to targeting non-conserved cysteines, for the development of selective covalent kinase inhibitors.

INTRODUCTION

The clinical successes of ibrutinib[1] and afatinib[2] have prompted a resurgence of interest in covalent drug discovery.[3,4] Covalent inhibitors can possess the advantages of increased potency, prolonged duration of action, decoupled pharmacodynamics and pharmacokinetics, and, often, require less frequent and lower doses.[4,5]

In the kinase field, researchers commonly target cysteine residues for covalent inhibition.[6] Targeted residues are often "non-catalytic and poorly conserved"[7] to maximise selectivity, and mitigate the risk of off-target covalent interactions.[4,5,7,8] However, only ~200 of over 500 human kinases have been mapped with a cysteine in the vicinity of the ATP pocket, and <50 have been demonstrated to covalently engage with inhibitors, restricting the scope of this strategy.[6,9–11] We chose to challenge this general approach by investigating the potential to selectively and irreversibly target the kinome-conserved lysine residue.[12] Covalent conjugation with lysine is far less common, due to its protonation state, and therefore poorer nucleophilicity under physiological conditions.[13] Nonetheless, interest in this nucleophile is rapidly gaining traction in the scientific community.[14–18]

The heterodimeric lipid kinase phosphoinositide 3-kinase delta (PI3Kδ)[19,20] has been targeted specifically over the related PI3Kα, β and γ isoforms for the treatment of a variety of diseases.[21,22] A number of selective reversible PI3Kδ small molecule inhibitors have entered clinical trials, with Zydelig recently obtaining FDA approval as a second-line treatment for relapsed follicular B-cell non-Hodgkin lymphoma, and relapsed chronic lymphocytic leukemia.[23–25] More recently, drug developers have targeted PI3Kδ for the treatment of inflammatory conditions such as asthma, chronic obstructive pulmonary disease (COPD), rheumatoid arthritis and activated PI3Kδ syndrome.[21,26–32]

To our knowledge, a selective covalent PI3Kδ inhibitor has not yet been disclosed, and there is no obvious isoform specific nucleophilic residue to target around the ATP binding site. Irreversible pan-PI3K inhibitors have been investigated previously, based on the fungal antibiotic wortmannin.[33–35] These compounds target the conserved lysine[12,36,37] for the covalent reaction, but are poorly selective.[35] Promiscuous kinase probes that covalently bind to this residue,[38–41] have also been developed and commercialised, however methods of selectively targeting this lysine in specific kinases have not yet been reported.

Herein we describe the development of the first selective, irreversible PI3Kδ inhibitor, which reacts with the conserved catalytic lysine (Lys779 in PI3Kδ numbering). Selectivity was achieved through optimisation of the reversible interactions in formation of the initial enzyme-

inhibitor complex, whilst the rate of the covalent reaction with the protein remained constant. The targeted lysine residue is present throughout the kinome, hence we anticipate that this strategy could provide an alternative general approach for the development of selective irreversible kinase inhibitors.

RESULTS AND DISCUSSION

Design of lysine targeting inhibitors. Clinical candidate **1** was identified as a suitable starting point due to its potency profile, and reversible interaction between the sulfonamide and Lys779.[23] We replaced the *cis*-dimethylmorpholine with the more basic, more soluble piperazine moiety[23] and hypothesised that substitution of the sulfonamide for an electrophilic functional group could afford covalent inhibitors (**Figure 1**). *In silico* modelling suggested that activated esters[42] would be tolerated in a reversible enzyme-inhibitor complex with PI3Kδ. Furthermore, the model of the covalently bound amide adduct that would form from these inhibitors did not reveal any obvious conformational issues (**Figure S1**).

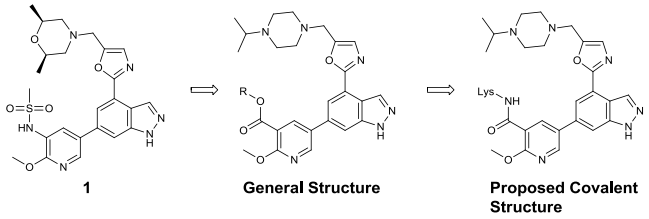

Figure 1. Generalised design principles for development of selective, irreversible PI3Kδ inhibitors.

Activated esters potently engage PI3Kδ in enzyme and cellular assays. A selection of phenolic esters were synthesised, and their potencies at PI3Kα, β, γ and δ were assessed using purified recombinant proteins via homogeneous time-resolved fluorescence (HTRF) assays.[23] Additionally, these compounds were tested in a phenotypic human-whole blood (hWB) assay, measuring reduction in interferon gamma (IFNγ) secretion after treatment with T-cell stimulating antibody, CytoStim, as a readout for PI3Kδ engagement[23] (**Table 1**).

Esters **2**-**7** potently inhibited PI3Kδ in isolated enzyme assays with pIC$_{50}$ values ranging from micromolar (ester **7**), to sub-nanomolar (ester **2**), confirming that the phenolic ester motifs were tolerated in the ATP binding pocket of the kinase. Furthermore, these data suggested a general trend that PI3Kδ potency of the inhibitors improved with the electron withdrawing ability of the R group attached to the ester, although the very high PI3Kδ activity of **2** was achieved at the expense of selectivity. The 4-trifluoromethylphenol ester **3** is an exception to this trend. Its relatively strong electron withdrawing effect (σ_p = 0.78, 0.54, 0.06 and -0.27 for NO_2, CF_3, F, and OMe substituents)[43] did not enhance the PI3Kδ potency compared to the electron neutral phenol **5**. The decreased potency of 2,4-dimethylphenol ester **7** may have arisen from clash between the 2-methyl group and the kinase, or steric hindrance to nucleophilic attack at the carbonyl. Compounds **3** to **5** showed the best profiles in this analysis, with biochemical potencies on-par with wortmannin **10**, and selectivity comparable to the FDA-approved PI3Kδ drug, Zydelig[24] **11**. Furthermore, compounds **3**-**5** provided good levels of inhibitory activity in the hWB assay (~10 nM), supporting engagement of PI3Kδ in cells, and were at least 15-fold more potent than **10** and **11** in this assay. It is worth noting that covalent inhibition is a time-dependent process, and the pIC$_{50}$ values would be expected to vary with time. The biochemical assays were read-out at 1 h in all cases, and the hWB assay at 20 h to provide consistency for data analysis.

Table 1. Compounds 2-9 inhibit PI3Kδ in biochemical and cellular assays.

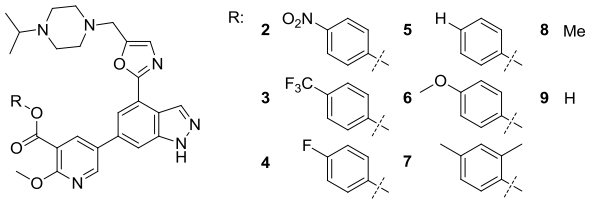

Cpd	pIC$_{50}$[a] δ	α	β	γ	hWB IFNγ pIC$_{50}$[b]
1	9.1	6.3	6.2	6.3	8.5
2	9.2[c]	8.2[c]	7.2[c]	5.8[c]	N.T
3	8.3	5.6	5.1	4.6	8.1
4	8.1	5.5	5.3	4.8	7.9
5	8.2	5.6	5.4	4.9	7.9
6	7.3	4.8	4.9	5.0	7.4
7	6.4	5.1	4.8	5.0	6.9
8	7.4	5.0	<4.5	<4.5	7.0
9	7.9	4.9	4.7	4.8	5.0
10 Wortmannin	8.3	8.1	8.0	8.2	6.7
11 Zydelig	8.1	5.0	5.8	6.6	6.7

[a]Biochemical pIC$_{50}$ data for all inhibitors at all four PI3K isoforms (measured after 1 h at K_M(ATP) using HTRF assays). [b]Phenotypic hWB pIC$_{50}$ derived from measuring levels of IFNγ after stimulation with CytoStim (20 h incubation, free compound concentrations are not available). Data for pan-covalent PI3K inhibitor wortmannin **10**, and FDA approved PI3Kδ selective, reversible inhibitor Zydelig **11** derived from these assays are also shown. [c]Compound found to be particularly unstable in DMSO, results reported from N = 2 only. N.T: Compound not tested due to instability of the DMSO 10 mM stock solution. All compounds were tested a minimum of three times in HTRF and hWB assays, with the exception of compounds **2**, **8** and **9** (**Table S1**).

Protein mass spectrometry and reactivity assessments indicated the potential for site-specific nucleophilic trapping by a lysine residue. After 5 min incubation of recombinant PI3Kδ with **4** (2:1 molar ratio of **4**:PI3Kδ), we observed formation of a single adduct by

intact protein liquid chromatography-mass spectrometry (LCMS). Compared to untreated protein, this mass shift was consistent with the addition of **4**, and loss of 4-fluorophenol. Repeating this assay with 10 molar equivalents of **4**, and 20 h incubation showed no additional adduct formation. Pre-incubation of PI3Kδ with 10 equivalents of the potent ATP-competitive reversible inhibitor[23] **12** prevented formation of the covalent adduct, suggesting covalent modification occurred in the ATP binding site. Carboxylic acid **9** showed no evidence of covalent bond formation in this experiment, implying that the phenolic ester was required for the covalent reaction. These results suggested that **4** was covalently, and specifically, binding to the ATP binding site of PI3Kδ (**Figure 2a**).

Reactivity analysis showed that **4** was stable to hydrolysis and reaction with *N*-Boc lysine under physiological conditions (phosphate buffer, pH 7.4, 37 °C), but upon deprotonation of the lysine smooth amide bond formation was observed (**Figures S2** and **S3**). Together with the mass spectrometry data suggesting that a single, specific modification occurred in the active site of PI3Kδ, we proposed that this bond could be forming with the conserved lysine.

Confirmation of Lys779 as the nucleophilic residue. After overnight soaking of pre-grown murine PI3Kδ crystals[20,23] with **4**, we observed a covalently bound adduct between the inhibitor and the targeted lysine residue (**Figure 2b**) by X-ray crystallography. Continuous electron density was seen between Lys779 and the carbonyl of the ester, and there was no evidence for the phenolic group being present, consistent with formation of an amide bond. Methyl ester **8** showed a reversibly bound adduct (**Figure S4**)**,** consistent with the reduced reactivity of this ester (**Figure S2**). The remainder of the compound satisfied the desired hydrogen bonding interactions between the indazole and hinge residues Val828 and Glu826, as well as occupying the selectivity region next to Trp760 with the basic amine.[23,44]

Time-course experiments to determine k_{inact} and K_I. Using the commercially available ADP Quest™ assay kit[45] we derived the concentration of inhibitor required for half of the maximum rate of covalent bond formation (K_I), the rate constant for irreversible inactivation (k_{inact}) and the second order rate constant typically used to characterise irreversible inhibitors (k_{inact}/K_I) (**Figure 2f**).[4,46–48] Full analyses for esters **2**-**7** and **10**, including equations used, are detailed in the Supporting Information.

All six esters exhibited non-linear reaction progress curves (**Figure 2c** and **Figure S7**) indicating time-dependent inhibition of PI3Kδ, consistent with covalent inactivation. The k_{inact}/K_I ranking obtained from the replot method correlated well with the potencies obtained from the PI3Kδ biochemical and hWB assays (**Table 1** and **Figure S7**). The kinetic data were visualised by plotting k_{inact} as a function of K_I, as described by Schwartz *et al.* (**Figure 2e**).[49] This representation clearly showed that similar k_{inact} values were found for all six esters (1.4-fold difference across the series), but K_I differences spanned two orders of magnitude, from 40 nM (compound **2**) to 7.8 μM (compound **6**) (195-fold difference, **Figure 2f**). This indicated that the electronic nature of the phenolate leaving group (*i.e.* pK_a value), and therefore expected chemical reactivity/leaving group ability, does not correlate with the rate of the covalent inactivation in this system. Rather, there is a correlation with K_I, suggesting a more complex mechanism than the traditional two-step scheme depicted in **Figure 2e**. The differences in pIC_{50} between the esters in our biochemical assay must therefore be dictated by reversible interactions in formation of the initial enzyme-inhibitor complex and not the rate of the covalent reaction. We have proposed a reaction mechanism supporting these data, invoking additional steps to explain the dependence of K_I on pK_a (**Supplementary Discussion** and **Scheme S1**). Finally, our prior analysis of the chemical reactivity of **4** (**Figures S2** and **S3**) showed it to be inert to nucleophilic substitution under physiological conditions. This suggested that the elevated reactivity observed in these kinetic analyses was occurring specifically in the protein, and that the local microenvironment around Lys779 may be contributing to an increased reactivity of this residue, rendering it hyper-reactive.[16,37,50,51]

Selectivity, despite the conserved lysine, is driven by reversible interactions. To assess off-target covalent binding, jump dilution and kinetic measurements at two closely related PI3K isoforms (α and β) were carried out with **4**. All three enzymes were inactivated in the jump dilution experiment without competing ATP indicating that **4** could covalently inhibit PI3Kα, β and δ at high pre-incubation concentrations (**Table S3**), without a competing ligand (**Figure 3a**). As controls, the experiment was performed with covalent pan-PI3K inhibitor **10**, and reversibly bound ester analogues **8** and **9**. **10** showed covalent inactivation of all three kinases, whereas **8** and **9** showed the expected regeneration of enzyme activity after dilution, consistent with a reversible mode of inhibition (**Figure 3a** and **Table S4**).

However, in the kinetic analysis with competing ATP (1 mM), linear reaction progressions were observed at PI3Kα and β at all tested concentrations (**Table S6**). The gradient of these plots decreased with increasing concentration of inhibitor, consistent with a rapid onset of inhibition. The absence of the slow-binding non-linear phase we had observed at PI3Kδ suggested no covalent binding was occurring at these kinases under these conditions. Indeed, for ester **4**, the kinetics at PI3Kδ reflected **10**, whilst the kinetics at PI3Kα and β reflected the reversibly bound methyl ester **8** (**Figure 3b**). This absence of apparent covalent adduct formation at PI3Kα and β was seen up to 8.5 μM of **4**, ~5x the PI3Kδ IC_{99} (= 1.59 μM) under these conditions. Reprocessing the raw data along the time axis allowed derivation of IC_{50} values every 30 s over this time window. These plots showed a time-dependent decrease in IC_{50} at PI3Kδ, but not at PI3Kα and β for **4** (**Figure S8**), supporting selective covalent inhibition in this assay. **4** also exhibited excellent selectivity against a panel of 10 lipid kinases and 140 protein kinases (**Tables S7** and **S8**).

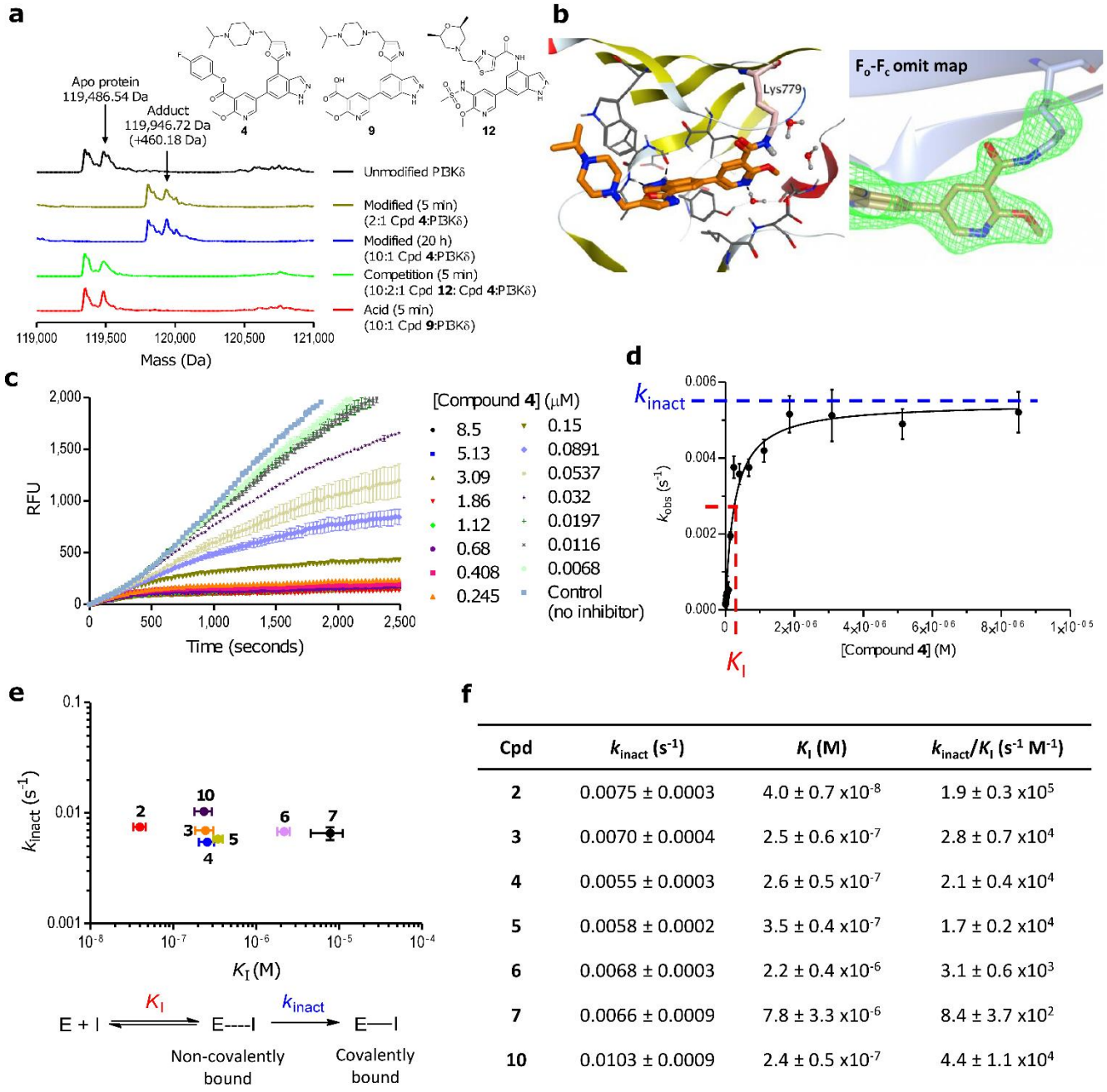

Cpd	k_{inact} (s^{-1})	K_I (M)	k_{inact}/K_I (s^{-1} M^{-1})
2	0.0075 ± 0.0003	4.0 ± 0.7 x10^{-8}	1.9 ± 0.3 x10^{5}
3	0.0070 ± 0.0004	2.5 ± 0.6 x10^{-7}	2.8 ± 0.7 x10^{4}
4	0.0055 ± 0.0003	2.6 ± 0.5 x10^{-7}	2.1 ± 0.4 x10^{4}
5	0.0058 ± 0.0002	3.5 ± 0.4 x10^{-7}	1.7 ± 0.2 x10^{4}
6	0.0068 ± 0.0003	2.2 ± 0.4 x10^{-6}	3.1 ± 0.6 x10^{3}
7	0.0066 ± 0.0009	7.8 ± 3.3 x10^{-6}	8.4 ± 3.7 x10^{2}
10	0.0103 ± 0.0009	2.4 ± 0.5 x10^{-7}	4.4 ± 1.1 x10^{4}

Figure 2. Compounds **2-7** covalently inactivate PI3Kδ by amide bond formation to Lys779, with potency dependent on reversible recognition. (a) Protein mass spectrometry. Top to bottom – apo protein; protein treated with two equivalents of **4**, analysed at 5 min; protein treated with 10 equivalents of **4** overnight; protein pre-treated with 10 equivalents of **12** for 15 min, prior to addition of two equivalents of **4**, and analysed at 5 min; protein incubated with 10 equivalents of **9** and analysed at 5 min. (b) Left: Crystal structure of **4** after overnight soaking with PI3Kδ crystals (PDB: 6EYZ). Right: F_o-F_c omit map is shown in green at 2.7 rmsd, with Lys799 side-chain and ligand co-ordinates removed, showing clear electron density from Lys779 onto the ligand. (c) Raw time-course data for **4**. Concentrations are shown after correction for absolute stock concentration using quantitative NMR (**Table S5**). (d) Plot of derived k_{obs} from (b) vs concentration of inhibitor to derive K_I and k_{inact}. (e) Plot of derived k_{inact} vs K_I for all 6 esters, and wortmannin.[4,46] (f) Table of k_{inact}, K_I and k_{inact}/K_I values. Kinetic measurements were performed in triplicate, and data are shown as the mean ± s.e.m.

These kinetic and jump dilution analyses revealed a concentration window where **4** covalently inactivated PI3Kδ, but not highly homologous isoforms of the same family, despite the conserved nature of the nucleophilic amino acid. Upon saturating the ATP binding site with high concentrations of inhibitor, in the absence of competing ATP, covalent inactivation does occur. However, in a cell-like environment, covalent inactivation of PI3Kα and β is unlikely to occur up to 5x the PI3Kδ IC_{99}. Consistent with our

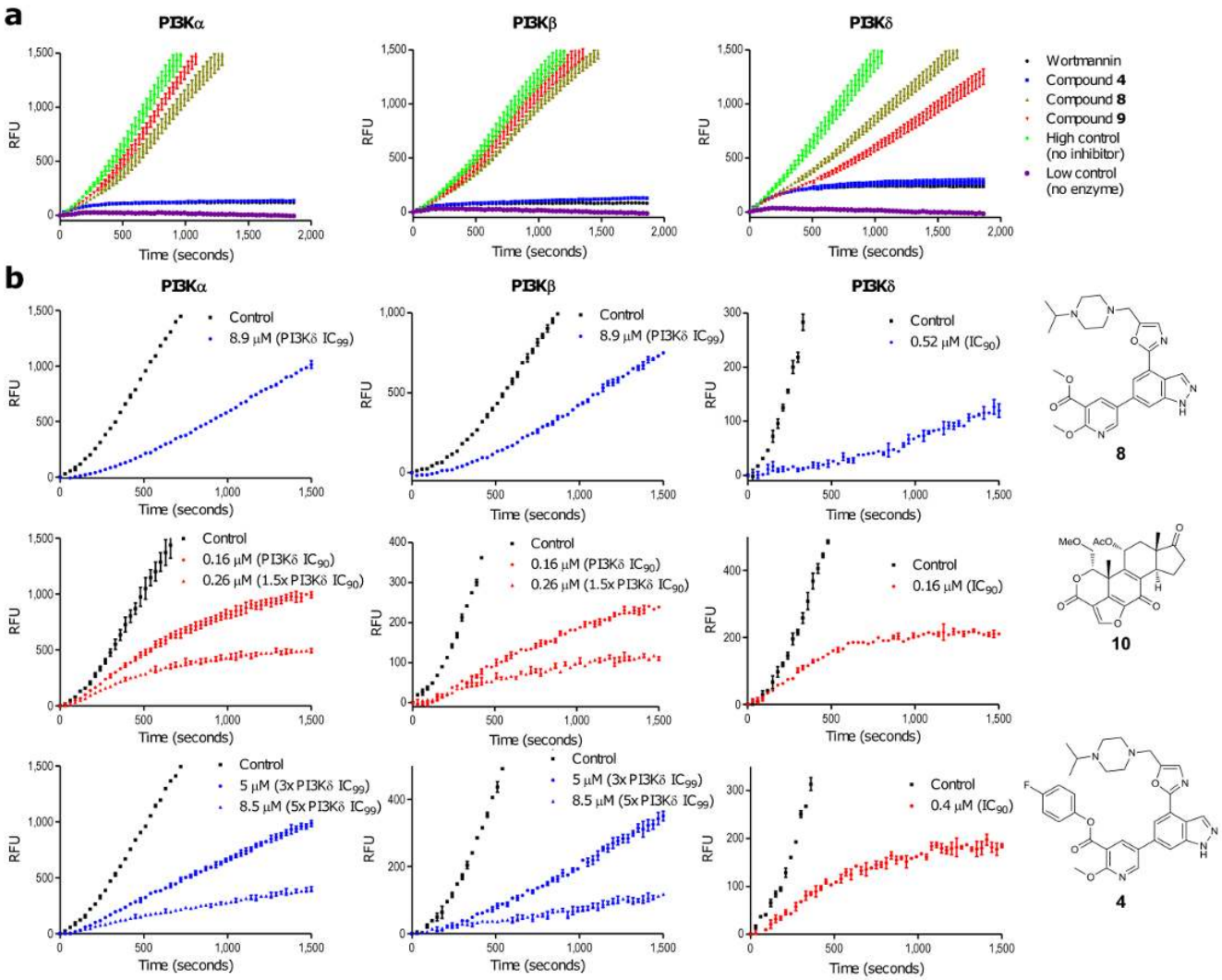

Figure 3. 4 does not covalently inhibit PI3Kα and β up to 5x PI3Kδ IC_{99} with cellular concentrations of ATP. (a) Jump dilutions conducted at PI3Kα (left), PI3Kβ (middle) and PI3Kδ (right) in the absence of competing ATP. Covalent inactivation of all three kinases was observed under these conditions by **4**. Inhibitor assays were conducted in triplicate and controls in duplicate. Results are plotted as mean ± s.e.m (b) Kinetic plots of the inhibition over time under saturating ATP conditions (1 mM). Linear plots (blue) relative to no-inhibitor controls (black) are typical of reversible inhibitors. Non-linear plots (red) relative to no-inhibitor controls (black) are typical of slow-binding inhibitors (confirmed to be irreversible by jump dilution experiments in (a)). The top row depicts reversible ester **8**, showing linear progress at IC_{90} at PI3Kδ, and at PI3Kα and β at the PI3Kδ IC_{99}. Middle row depicts irreversible inactivation of all three kinases by wortmannin at IC_{90} for PI3Kδ (1.5x PI3Kδ IC_{90} curves are also shown). Bottom row shows selective ester **4**, exhibiting covalent inhibition at PI3Kδ at IC_{90}, and reversible inhibition at PI3Kα and β at 3x and 5x PI3Kδ IC_{99}. Assays were conducted in duplicate, and results are shown as mean ± s.e.m.

earlier observation that potency differences between the esters at PI3Kδ was governed by reversible interactions, this selectivity must also arise from differences in the initial reversible binding interactions (K_I) with these kinases.

Chemoproteomics revealed 4 to be selective for PI3Kδ in live cells. Azido probe **13** was synthesised, and retained potency at PI3Kδ in the biochemical HTRF assay (pIC_{50} = 7.6). At 1 μM, it was shown to covalently modify a protein with a molecular weight consistent with PI3Kδ in THP-1 monocyte lysates by in-gel fluorescence after strain-promoted azide-alkyne cycloaddition click reaction (SPAAC) with dibenzycyclooctyne-conjugated-Cy5 dye (DBCO-Cy5), and SDS-PAGE separation. Co-elution of PI3Kδ with the Cy5 signal was confirmed by immunostaining with p110δ antibody after transfer to PVDF membranes (**Figure S9**).[52] Furthermore, the Cy5 fluorescence signal was gradually ablated in the presence of increasing concentrations of **4**, with a pIC_{50} of 7.5, suggesting potent engagement of PI3Kδ by **4** in complex cell lysates.

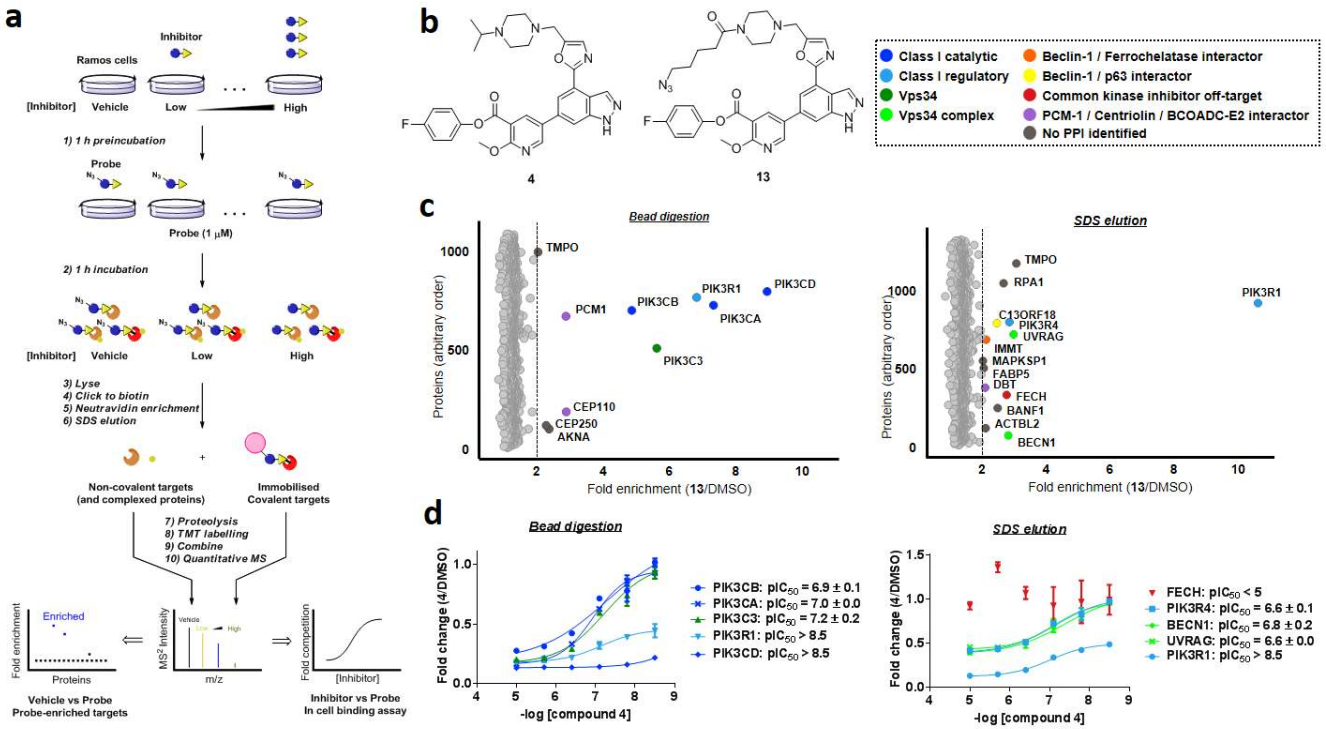

Figure 4. Chemoproteomic analysis identifies targets of **4** in human cells. (a) General assay design. (b) Structures of **4** and **13**, and key for graphs below. (c) The scatter plots display proteins enriched with neutravidin beads after clicking a biotin moiety to proteins labeled *in situ* with probe **13** (1 μM) relative to vehicle control. Proteins were accessed by enzymatic bead digestion or SDS elution from the bead. The dotted lines represent 2-fold enrichment (**13**/DMSO) and proteins with >2-fold enrichment are deemed specific targets of **13**, and are labeled by their entrez gene ID. (d) Dose-response curves for competition of **13** binding to specifically enriched targets after pretreatment of cells for 1 h with **4**. Binding curves and resulting *p*IC50 values are shown for proteins enriched >2-fold. With the exception of FECH, values are not plotted if no binding curve could be fitted using GraphPad Prism 7.03. The values represented are the average ± s.e.m. from two biological replicates. In (c) and (d), data were filtered with the criteria that quantified unique peptide matches > 1 and quantified unique peptide to spectra matches >2. Proteins were required to be identified and quantified in both replicates to be included in the analysis, and data are plotted as the mean of the TMT label ratios (MS^2) for the three most abundant peptides (MS^1) per protein.

Protein targets of probe **13** in Ramos cells were then identified by a quantitative mass spectrometry-based chemoproteomics method using tandem mass tag (TMT) labelling (**Figure 4a**), based on related experiments by Lanning *et al*[53] and Niessen *et al*.[54] Cells were treated with either vehicle or **13** at 1 μM for 1 h, lysed, and proteins bound by **13** were enriched with neutravidin beads after SPAAC reaction with a DBCO-biotin conjugate. Non-covalently bound proteins were expected to be predominantly eluted with SDS, whereas covalent targets should only be detected after on-bead proteolysis.

Comparison to vehicle-treated cells identified 22 out of ~1000 identified proteins that were specifically enriched >2-fold by *in situ* treatment with **13** (**Figure 4c** and **Supplementary Data Set**). Of those 22 proteins, eight were exclusively identified after direct proteolysis, including the class I catalytic subunits of PI3Kδ (gene ID PIK3CD), PI3Kα (gene ID PIK3CA), PI3Kβ (gene ID PIK3CB), and the class III PI3K protein Vps34 (gene ID PIK3C3), suggesting these proteins as covalent targets of **13**. In contrast, the Vps34 regulatory subunits[55] PI3K regulatory subunit 4 (gene ID PIK3R4), Beclin-1 (gene ID BECN1), p63 (gene ID UVRAG), mitofilin (gene ID IMMT), and protein RUBCNL-like (gene ID C13ORF18) as well as the common kinase inhibitor off-target ferrochelatase[56] (gene ID FECH), were only found in the SDS eluates. The possibility to elute those proteins from the capturing matrix with SDS buffer implicates those proteins as reversible binders of **13**, or proteins in complexes with enriched targets. The PI3K regulatory subunit α (gene ID PIK3R1) was identified in the bead digest fraction as well as in the SDS eluates. Signal abundances of detected tryptic peptides (MS^1 intensities) indicated a 3 to 4-fold higher abundance in the SDS fraction than in the bead digests. This suggests major, but incomplete, elution of this known interactor of class I catalytic PI3K subunits[26] with the applied conditions.

To accurately assess off-target interactions of **4**, we derived dose-response curves from competing the binding to **13** by pretreatment with concentrations of **4** ranging from 10 μM to 3.2 nM for 1 h (**Figure 4d**). For the specifically enriched proteins exclusively found in the bead digests, we calculated pIC_{50} values for PI3Kδ, PI3Kα, PI3Kβ, and hVps34 to be > 8.5, 7.0, 6.9 and 7.2, respectively. This indicates that irreversible binding of PI3Kδ to **13** can be competed by **4** with >20-fold selectivity at the used incu-

bation conditions. For the proteins identified exclusively in the SDS fraction, we determined reasonable binding curves for Beclin-1, p63, and PI3K regulatory subunit 4. All resulted in very similar pIC_{50} values ($pIC_{50,BECN1}$ = 6.8; $pIC_{50,UVRAG}$ = 6.6; $pIC_{50,PIK3R4}$ = 6.6). Binding curves were incomplete for those proteins (maximal competition by 10 μM compound c.a. 50%), suggesting they were interacting with a known complex partner,[55] rather than being true targets of the compound. A similar effect might be observed for PI3K regulatory subunit α for which a pIC_{50} value >8.5 was determined. As a complex partner of PI3Kα, PI3Kβ, and PI3Kδ,[26] the determined apparent dose-dependent competition may result from a combination of competitive binding to any of these PI3K proteins. Within the tested concentration range, mitofilin, ferrochelatase, and protein RUBCNL-like, (as well as the remaining proteins that were specifically enriched with **13**) did not show strong competition of binding by **4**, suggesting low affinity binding.

These chemoproteomic data support minimal off-target binding by **4** in human cells. Coupled with our selectivity hypothesis and kinase panel investigations above (**Figure 3** and **Tables S7** and **S8**), we propose **4** to be a highly selective irreversible inhibitor of PI3Kδ at concentrations below 1 μM.

Cellular washout studies suggest an extended duration of action. CD4+ T cells were incubated with **4** or **12** (hWB pIC_{50} = 7.9) for 2 h, then washed and incubated for a further 48 h before stimulation with αCD3 and measurement of IFNγ release. **4** showed sustained depletion of IFNγ secretion 48 h after washout, without cytotoxic effects (**Figure S10**), whereas regeneration of IFNγ secretion was observed for **12** (**Figure 5**). These results, taken together with the data presented above, suggest that inhibition of PI3Kδ could be sustained for at least 48 h using an irreversible targeting approach, with no cytotoxic effect. It is worth noting, however, that cellular accumulation of dibasic piperazines could also be a contributing factor to the duration of action for this series of compounds.[57,58]

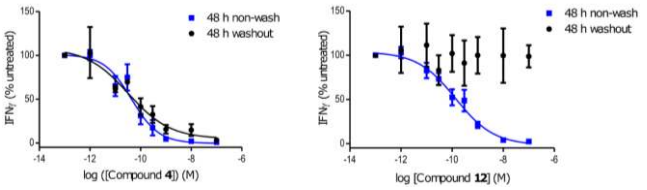

Figure 5. Inhibitor **4** showed a prolonged duration of action, up to at least 48 h in CD4+ T cells. Cellular washout studies conducted in CD4+ T cells isolated from hWB. Cells were treated with inhibitors for 2 h, washed, and stimulated with αCD3 to induce IFNγ release, measured after 48 h. Left: Covalent compound **4** showed a clear sustained duration of action (black circles) 48 h after washing. Right: Reversible compound **12** showed a clear disruption of the inhibition profile (black circles) 48 h after washing. The experiment was repeated using 5 donors (for each donor: N = 3 replicates for washout, and N = 2 replicates for non-wash condition), and results are depicted as mean ± s.e.m. Non-washed curves showing the dose-response after 48 h are shown in blue.

CONCLUSION

Selective covalent inhibition relies on a two step process of reversible binding and then covalent inactivation.[4,5] Here, we have demonstrated that selectivity in formation of the initial enzyme-inhibitor complex is the crucial factor for achieving potent, selective covalent inhibition of conserved residues. Kinetic studies indicated that the electronics, and expected chemical reactivities, of the electrophilic esters did not affect the rate of covalent bond formation with the enzyme, k_{inact}. The observed variation in potency of the esters at PI3Kδ (**Table 1**) therefore arose from the reversible binding steps of the inhibitors, due to electronic changes in the phenolic group, reflected by K_I. Furthermore, through kinetic studies at PI3Kα, β, and δ we determined that there was a reasonable concentration range at which covalent inhibition of PI3Kδ could be achieved, without covalent inactivation of related enzymes. This was confirmed by chemoproteomic studies with **13** *in situ* which suggested minimal off-target binding of **4**, and a >20-fold selectivity window for covalent modification of PI3Kδ, despite conservation of the targeted lysine residue and presence of other reactive moieties.

As a more general approach, variation of the electrophilic centre to affect reversible binding could be exploited for fine-tuning of the potency, selectivity, and physicochemical properties of inhibitors for irreversible drug discovery programmes. By maintaining a constant k_{inact} across a series of electrophilic esters, this provides an orthogonal approach to established EGFR and Janus Kinase (JAK) inhibitors that vary the k_{inact} to improve the drug profile.[8,59] Furthermore, a common method for enzymes to develop resistance to covalent inhibitors targeting poorly conserved cysteines is by point mutation of the modified residue.[60] A similar resistance mechanism would not be applicable to the strategy we have developed, as mutation of the catalytic lysine would render the kinase inactive.[61] Finally, the potential lability of these esters could impart kinetic selectivity *in vivo*. Zaro *et al.* recently described how the proteome-wide selectivity of ibrutinib improved when a fumarate ester was incorporated into the covalent warhead. They attributed this to hydrolysis of the metabolically labile ester, affording an inert 1,4-unsaturated carboxylate.[62] Carboxylic acid **9** formed in our case is poorly active in the cellular assay (pIC_{50} = 5.0, **Table 1**), and inert to covalent bond formation by mass-spectrometry (**Figure 2a**), suggesting a similar mechanism could be observed here.

By modification of a known reversible inhibitor,[23] we have developed a series of esters which selectively and covalently inhibit PI3Kδ. In addition to the excellent selectivity profile, our lead compound **4** showed ~10 nM activity in the hWB phenotypic inflammatory cytokine response assay, and extended duration of action (>48 h), in cellular washout studies. Owing to the importance of

PI3Kδ as a target for inflammation and oncology, this selective, covalent PI3Kδ inhibitor could have applications in the development of long-acting therapeutics.

Prior studies have shown that the targeted conserved lysine reacts covalently with promiscuous probes possessing reactive warheads.[38–41] We therefore envisage that this approach could be orthogonal to non-conserved cysteine targeting, and applicable across the kinome. By this method, researchers may be able to generate selective covalent chemical probes of any chosen kinase, which could provide tools to vastly improve the understanding of human biology in diseased states.

ASSOCIATED CONTENT

Supporting Information.
Biological methods, synthetic methods and characterisation, supplementary figures, supplementary tables, supplementary mass-spectrometry tables, and supplementary discussions.

AUTHOR INFORMATION

Corresponding Author

* sebastien.x.campos@gsk.com

Author Contributions

All authors have given approval to the final version of the manuscript.

Notes

The authors declare no competing financial interests.

ACKNOWLEDGMENT

We thank the GlaxoSmithKline/University of Strathclyde Industrial PhD programme for funding this work. We also thank D. House for providing revisions of the manuscript, J.N. Hamblin and V. Patel for intellectual discussions, and N. Barton, C. Chitty, P. Francis, L. Gordon, N. Hodnett, S. Kumper, S.M. Lynn, J.E. Rowedder, E. Sherriff and H. Taylor for technical assistance and discussion.

REFERENCES

(1) Kim, E. S.; Dhillon, S. *Drugs* **2015**, *17*, 769–776.
(2) Hossam, M.; Lasheen, D. S.; Abouzid, K. A. M. *Arch. Pharm. Chem. Life Sci.* **2016**, *349*, 1–21.
(3) Bradshaw, J. M.; McFarland, J. M.; Paavilainen, V. O.; Bisconte, A.; Tam, D.; Phan, V. T.; Romanov, S.; Finkle, D.; Shu, J.; Patel, V.; Ton, T.; Li, X.; Loughhead, D. G.; Nunn, P. A.; Karr, D. E.; Gerritsen, M. E.; Funk, J. O.; Owens, T. D.; Verner, E.; Brameld, K. A.; Hill, R. J.; Goldstein, D. M.; Taunton, J. *Nat. Chem. Biol.* **2015**, *11*, 525–531.
(4) Singh, J.; Petter, R. C.; Baillie, T. A.; Whitty, A. *Nat. Rev. Drug Discov.* **2011**, *10*, 307–317.
(5) Baillie, T. A. *Angew. Rev.* **2016**, 55, 2–17.
(6) Liu, Q.; Sabnis, Y.; Zhao, Z.; Zhang, T.; Buhrlage, S. J.; Jones, L. H.; Gray, N. S. *Chem. Biol.* **2013**, *20*, 146–159.
(7) Mah, R.; Thomas, J. R.; Shafer, C. M. *Bioorganic Med. Chem. Lett.* **2014**, *24*, 33–39.
(8) Nacht, M.; Qiao, L.; Sheets, M. P.; Martin, T. S.; Labenski, M.; Mazdiyasni, H.; Karp, R.; Zhu, Z.; Chaturvedi, P.; Bhavsar, D.; Niu, D.; Westlin, W.; Petter, R. C.; Medikonda, A. P.; Singh, J. *J. Med. Chem.* **2013**, *56*, 712–721.
(9) Zhang, J.; Yang, P. L.; Gray, N. S. *Nat. Rev. Cancer* **2009**, *9*, 28–39.
(10) Leproult, E.; Barluenga, S.; Moras, D.; Wurtz, J.-M.; Winssinger, N. *J. Med. Chem.* **2011**, *54*, 1347–1355.
(11) Zhao, Z.; Liu, Q.; Bliven, S.; Xie, L.; Bourne, P. E. *J. Med. Chem.* **2017**, *60*, 2879–2889.
(12) Carrera, A. C.; Alexandrov, K.; Roberts, T. M. *Proc. Natl. Acad. Sci. U. S. A.* **1993**, *90*, 442–446.
(13) Dahal, U.; Gilbert, A.; Obach, R.; Chen, J.; Garcia-Irizarry, C.; Schuff, B.; Starr, J.; Uccello, D.; Young, J. *Med. Chem. Commun.* **2016**, *7*, 864–872.
(14) Akçay, G.; Belmonte, M. A.; Aquila, B.; Chuaqui, C.; Hird, A. W.; Lamb, M. L.; Rawlins, P. B.; Su, N.; Tentarelli, S.; Grimster, N. P.; Su, Q. *Nat. Chem. Biol.* **2016**, *12*, 931–936.
(15) Anscombe, E.; Meschini, E.; Mora-vidal, R.; Stephen, R.; Endicott, J. A.; Griffin, R. J. *Chem. Biol.* **2015**, *22*, 1159–1164.
(16) Hacker, S. M.; Backus, K. M.; Lazear, M. R.; Forli, S.; Correia, B. E.; Cravatt, B. F. *Nat. Chem.* **2017,** DOI: http://dx.doi.org/10.1038/nchem.2826
(17) Pettinger, J.; Jones, K.; Cheeseman, M. D. *Angew. Chemie Int. Ed.* **2017**. DOI: 10.1002/anie.201707630
(18) Pettinger, J.; Bihan, Y.-V. Le; Widya, M.; Montfort, R. L. M. Van; Jones, K.; Cheeseman, M. D. *Angew. Chemie Int. Ed.* **2017**, *56*, 3536–3540.
(19) Cantley, L. L. C. *Science* **2002**, *296*, 1655–1657.
(20) Berndt, A.; Miller, S.; Williams, O.; Le, D. D.; Houseman, B. T.; Pacold, J. I.; Gorrec, F.; Hon, W.-C.; Liu, Y.; Rommel, C.; Gaillard, P.; Rückle, T.; Schwarz, M. K.; Shokat, K. M.; Shaw, J. P.; Williams, R. L. *Nat. Chem. Biol.* **2010**, *6*, 117–124.
(21) Stark, A.-K.; Sriskantharajah, S.; Hessel, E. M.; Okkenhaug, K. *Curr. Opin. Pharmacol.* **2015**, *23*, 82–91.
(22) Fruman, D. A.; Chiu, H.; Hopkins, B. D.; Bagrodia, S.; Cantley, L. C.; Abraham, R. T. *Cell* **2017**, *170*, 605–635.
(23) Down, K.; Amour, A.; Baldwin, I. R.; Cooper, A. W. J.; Deakin, A. M.; Felton, L. M.; Guntrip, S. B.; Hardy, C.; Harrison, Z. A.; Jones, K. L.; Jones, P.; Keeling, S. E.; Le, J.; Livia, S.; Lucas, F.; Lunniss, C. J.; Parr, N. J.; Robinson, E.; Rowland, P.; Smith, S.; Thomas, D. A.; Vitulli, G.; Washio, Y.; Hamblin, J. N. *J. Med. Chem.* **2015**, *58*, 7381–7399.
(24) Somoza, J. R.; Koditek, D.; Villaseñor, A. G.; Novikov, N.; Wong, M. H.; Liclican, A.; Xing, W.; Lagpacan, L.; Wang, R.; Schultz, B. E.; Papalia, G. A.; Samuel, D.; Lad, L.; McGrath, M. E. *J. Biol. Chem.* **2015**, *290*, 8439–8446.
(25) Liu, P.; Cheng, H.; Roberts, T. M.; Zhao, J. J. *Nat. Rev. Drug Discov.* **2009**, *8*, 627–644.
(26) Vanhaesebroeck, B.; Whitehead, M. A.; Piñeiro, R. *J. Mol. Med.* **2016**, *94*, 5–11.
(27) Rowan, W. C.; Smith, J. L.; Affleck, K.; Amour, A. *Biochem. Soc. Trans.* **2012**, *40*, 240–245.
(28) Rommel, C.; Camps, M.; Ji, H. *Nat. Rev. Immunol.* **2007**, *7*, 191–201.
(29) Koyasu, S. *Nat. Immunol.* **2003**, *4*, 313–319.
(30) Ghigo, A.; Damilano, F.; Braccini, L.; Hirsch, E. *BioEssays* **2010**, *32*, 185–196.
(31) Okkenhaug, K.; Bilancio, A.; Farjot, G.; Priddle, H.; Sancho, S.; Peskett, E.; Pearce, W.; Meek, S. E.; Salpekar, A.; Waterfield, M. D.; Smith, A. J. H.; Vanhaesebroeck, B. *Science* **2002**, *297*, 1031–1034.
(32) Puri, K. D.; Doggett, T. A.; Douangpanya, J.; Hou, Y.; Tino, W. T.; Wilson, T.; Graf, T.; Clayton, E.; Turner, M.; Hayflick, J. S.; Diacovo, T. G. *Blood* **2004**, *103*, 3448–3456.
(33) Norman, B. H.; Shih, C.; Toth, J. E.; Ray, J. E.; Dodge, J. a.; Johnson, D. W.; Rutherford, P. G.; Schultz, R. M.; Worzalla, J. F.; Vlahos, C. J. *J. Med. Chem.* **1996**, *39*, 1106–1111.
(34) Waterfield, M. D.; Panayotou, G.; Wymann, M. P.; Bulgarelli-Leva, G.; Zvelebil, M. J.; Pirola, L.; Vanhaesebroeck, B. *Mol. Cell. Biol.* **1996**, *16*, 1722–1733.
(35) Hong, D. S.; Bowles, D. W.; Falchook, G. S.; Messersmith, W. A.; George, G. C.; O'Bryant, C. L.; Vo, A. C. H.; Klucher, K.; Herbst, R. S.; Eckhardt, S. G.; Peterson, S.; Hausman, D. F.; Kurzrock, R.; Jimeno, A. *Clin. Cancer Res.* **2012**, *18*, 4173–4182.
(36) Walker, E. H.; Pacold, M. E.; Perisic, O.; Stephens, L.; Hawkins, P. T.; Wymann, M. P.; Williams, R. L. *Mol. Cell*

2000, *6*, 909–919.
(37) Miller, R. M.; Taunton, J. *Methods Enzymol.* **2014**, *548*, 93–116.
(38) Patricelli, M. P.; Nomanbhoy, T. K.; Wu, J.; Brown, H.; Zhou, D.; Zhang, J.; Jagannathan, S.; Aban, A.; Okerberg, E.; Herring, C.; Nordin, B.; Weissig, H.; Yang, Q.; Lee, J. D.; Gray, N. S.; Kozarich, J. W. *Chem. Biol.* **2011**, *18*, 699–710.
(39) Cravatt, B. F.; Wright, A. T.; Kozarich, J. W. *Annu. Rev. Biochem.* **2008**, *77*, 383–414.
(40) Zhao, Q.; Ouyang, X.; Wan, X.; Gajiwala, K. S.; Kath, J. C.; Jones, L. H.; Burlingame, A. L.; Taunton, J. *J. Am. Chem. Soc.* **2017**, *139*, 680–685.
(41) Patricelli, M. P.; Szardenings, A. K.; Liyanage, M.; Nomanbhoy, T. K.; Wu, M.; Weissig, H.; Aban, A.; Chun, D.; Tanner, S.; Kozarich, J. W. *Biochemistry* **2007**, *46*, 350–358.
(42) Choi, S.; Connelly, S.; Reixach, N.; Wilson, I. A.; Kelly, J. W. *Nat. Chem. Biol.* **2010**, *6*, 133–139.
(43) Hansch, C.; Leo, A.; Taft, R. W. *Chem. Rev.* **1991**, *91*, 165–195.
(44) Sutherlin, D. P.; Baker, S.; Bisconte, A.; Blaney, P. M.; Brown, A.; Chan, B. K.; Chantry, D.; Castanedo, G.; Depledge, P.; Goldsmith, P.; Goldstein, D. M.; Hancox, T.; Kaur, J.; Knowles, D.; Kondru, R.; Lesnick, J.; Lucas, M. C.; Lewis, C.; Murray, J.; Nadin, A. J.; Nonomiya, J.; Pang, J.; Pegg, N.; Price, S.; Reif, K.; Safina, B. S.; Salphati, L.; Staben, S.; Seward, E. M.; Shuttleworth, S.; Sohal, S.; Sweeney, Z. K.; Ultsch, M.; Waszkowycz, B.; Wei, B. *Bioorganic Med. Chem. Lett.* **2012**, *22*, 4296–4302.
(45) Charter, N. W.; Kauffman, L.; Singh, R. A. J.; Eglen, R. M. *J. Biomol. Screen.* **2006**, *11*, 390–399.
(46) Copeland, R. A. *Enzymes: A Practical Introduction to Structure, Mechanism and Data Analysis*, Ch. 10 (Wiley, New York, NY, USA, 2000)
(47) Kitz, R.; Wilson, B. *J. Biol. Chem.* **1962**, *237*, 3245–3249.
(48) Strelow, J. M. *SLAS Discov.* **2017**, *22*, 3–20.
(49) Schwartz, P. A.; Kuzmic, P.; Solowiej, J.; Bergqvist, S.; Bolanos, B.; Almaden, C.; Nagata, A.; Ryan, K.; Feng, J.; Dalvie, D.; Kath, J. C.; Xu, M.; Wani, R.; Murray, B. W. *Proc. Natl. Acad. Sci. U. S. A.* **2014**, *111*, 173–178.
(50) Weerapana, E.; Wang, C.; Simon, G. M.; Richter, F.; Khare, S.; Dillon, M. B. D.; Bachovchin, D. A.; Mowen, K.; Baker, D.; Cravatt, B. F. *Nature* **2010**, *468*, 790–795.
(51) Backus, K. M.; Correia, B. E.; Lum, K. M.; Forli, S.; Horning, B. D.; González-Páez, G. E.; Chatterjee, S.; Lanning, B. R.; Teijaro, J. R.; Olson, A. J.; Wolan, D. W.; Cravatt, B. F. *Nature* **2016**, *534*, 570–574.
(52) Rutkowska, A.; Thomson, D. W.; Vappiani, J.; Werner, T.; Mueller, K. M.; Dittus, L.; Krause, J.; Muelbaier, M.; Bergamini, G.; Bantscheff, M. *ACS Chem. Biol.* **2016**, *11*, 2541–2550.
(53) Lanning, B. R.; Whitby, L. R.; Dix, M. M.; Douhan, J.; Gilbert, A. M.; Hett, E. C.; Johnson, T. O.; Joslyn, C.; Kath, J. C.; Niessen, S.; Roberts, L. R.; Schnute, M. E.; Wang, C.; Hulce, J. J.; Wei, B.; Whiteley, L. O.; Hayward, M. M.; Cravatt, B. F. *Nat. Chem. Biol.* **2014**, *10*, 760–767.
(54) Niessen, S.; Dix, M. M.; Barbas, S.; Hayward, M. M.; Kath, J. C.; Cravatt, B. F.; Niessen, S.; Dix, M. M.; Barbas, S.; Potter, Z. E.; Lu, S.; Brodsky, O. *Cell Chem. Biol.* **2017**, *24*, 1–13.
(55) Yu, X.; Long, Y. C.; Shen, H. M. *Autophagy* **2015**, *11*, 1711–1728.
(56) Klaeger, S.; Gohlke, B.; Perrin, J.; Gupta, V.; Heinzlmeir, S.; Helm, D.; Qiao, H.; Bergamini, G.; Handa, H.; Savitski, M. M.; Bantscheff, M.; Médard, G.; Preissner, R.; Kuster, B. *ACS Chem. Biol.* **2016**, *11*, 1245–1254.
(57) Cahn, A.; Hamblin, J. N.; Begg, M.; Wilson, R.; Dunsire, L.; Sriskantharajah, S.; Montembault, M.; Leemereise, C. N.; Galinanes-Garcia, L.; Watz, H.; Kirsten, A. M.; Fuhr, R.; Hessel, E. M. *Pulm. Pharmacol. Ther.* **2017**, *46*, 69–77.
(58) Kazmi, F.; Hensley, T.; Pope, C.; Funk, R. S.; Loewen, G. J.; Buckley, D. B.; Parkinson, A. *Drug Metab. Dispos.* **2013**, *41*, 897–905.
(59) Thorarensen, A.; Dowty, M. E.; Banker, M. E.; Juba, B. M.; Jussif, J.; Lin, T.; Vincent, F.; Czerwinski, R. M.; Casimiro-Garcia, A.; Unwalla, R.; Trujillo, J. I.; Liang, S.; Balbo, P.; Che, Y.; Gilbert, A. M.; Brown, M. F.; Hayward, M.; Montgomery, J.; Leung, L.; Yang, X.; Soucy, S.; Hegen, M.; Coe, J.; Langille, J.; Vajdos, F. F.; Chrencik, J. E.; Telliez, J.-B. *J. Med. Chem.* **2017**, *60*, 1971–1993.
(60) Engel, J.; Lategahn, J.; Rauh, D. *ACS Med. Chem. Lett.* **2016**, *7*, 2–5.
(61) Iyer, G. H.; Moore, M. J.; Taylor, S. S. *J. Biol. Chem.* **2005**, *280*, 8800–8807.
(62) Zaro, B. W.; Whitby, L. R.; Lum, K. M.; Cravatt, B. F. *J. Am. Chem. Soc.* **2016**, *138*, 15841–15844.